Journal of Alloys and Compounds 504S (2010) S82–S85

Contents lists available at ScienceDirect

Journal of Alloys and Compounds

journal homepage: www.elsevier.com/locate/jallcom

High temperature deformation behaviors of $Ti_{40}Zr_{25}Ni_3Cu_{12}Be_{20}$ bulk metallic glass

Yongjiang Huang[a,b,c,*], Jun Shen[a,c], Yi Sun[b], Jianfei Sun[a], John J.J. Chen[d]

[a] School of Materials Science and Engineering, Harbin Institute of Technology, Harbin 150001, China
[b] Department of Astronautics and Mechanics, Harbin Institute of Technology, Harbin 150001, China
[c] Key Laboratory of Micro-systems and Micro-structures Manufacturing (Harbin Institute of Technology), Ministry of Education, China
[d] Department of Chemical and Materials Engineering, University of Auckland, Auckland 1142, New Zealand

ARTICLE INFO

Article history:
Received 22 June 2009
Received in revised form 3 February 2010
Accepted 8 February 2010
Available online 3 March 2010

Keywords:
Ti-based bulk metallic glass
Superplastic deformation
Supercooled liquid region
Viscosity
Activation volume

ABSTRACT

Compressive deformation behaviors of a cast $Ti_{40}Zr_{25}Ni_3Cu_{12}Be_{20}$ bulk metallic glass in the test temperatures ranging from 428 to 658 K were examined in a broad range of strain rates from 1.3×10^{-4} to 3×10^{-2} s^{-1}. The alloy studied exhibits an extraordinary compressive superplastic formability within the supercooled liquid region, typically evidenced by a large compressive strain up to 0.83. The superplastic flow behaviors are strongly dependent on the test temperatures and applied strain rates. At low temperatures or high strain rates, the viscosity measured is found to dramatically decrease with increasing strain rate (i.e., non-Newtonian flow) and a stress overshoot is detected in the first steps of strain. At low strain rates or high test temperatures, the studied glass exhibits a Newtonian flow behavior. The value of activation volume increases with increasing test temperatures.

© 2010 Elsevier B.V. All rights reserved.

1. Introduction

During the last decades, bulk metallic glasses (BMGs) have stimulated extensive enthusiasm for scientific research because of their superior properties associated with their unique atomic structure, including high yield strength, large elastic limit, and excellent wear resistance [1,2]. However, widespread structural and functional applications of these advanced materials are severely hindered by the lack of significant permanent deformation prior to failure [3,4]. For BMG alloys, plastic deformation is highly localized into very narrow shear bands, resulting in no or very little plastic strain (usually less than 2%) and catastrophic failure at room temperature [3,4]. It is well documented that heating BMGs to temperatures between the glass transition (T_g) and crystallization (T_x) temperature (i.e., the so-called supercooled liquid region, SLR, or ΔT) caused them to soften drastically to a point at which they take on complex shapes unachievable with conventional metals [5–10]. Chiang et al. [8] found that $Cu_{60}Zr_{20}Hf_{10}Ti_{10}$ glass exhibited a large compressive strain of 0.78 when deformed within SLR. Gun et al. [9] demonstrated that elongations of over 1000% were possible during high temperature deformation of $Mg_{65}Cu_{25}Y_{10}$ BMG. Wang et al. [7] examined the superplastic deformation behaviors of Vit1 bulk glassy alloy and found that its maximum elongation can reach as high as 1624% within SLR. The unique superplastic formability within SLR might be able to circumvent this lack of room temperature ductility and has been used for a wide range of processes, including nano-moulding [11], net-shape fabrication [12,13], extrusion [10,14], surface embossing [15] and writing-erasing [16]. In the present study, the compressive deformation behaviors and formability of a Ti-based bulk metallic glass within SLR were examined.

2. Experimental details

A typical BMG, $Ti_{40}Zr_{25}Ni_3Cu_{12}Be_{20}$ (at.%), was chosen for this study, due to its excellent glass-forming ability [17,18]. To achieve compositional homogeneity, the master alloys were remelted at least four times. Alloy ingots were prepared by arc melting pure metals of Ti, Zr, Ni, Cu, and Be together in a Ti-gettered argon atmosphere. Cylindrical samples of the studied alloy with 3 mm in diameter were obtained by melt casting into a Cu mould. The amorphous structure of the as-cast samples was verified by X-ray diffraction. Thermal response was examined by differential scanning calorimetry (DSC) at a heating rate of 20 K min^{-1}. The DSC study revealed that T_g and T_x are 603 and 654 K, respectively, giving rise to a supercooled liquid region of 51 K. For a series of compressive mechanical tests, the 3 mm diameter cylindrical samples were cut into 6 mm lengths from the as-cast rods and then carefully ground and polished to ensure that both the top and the bottom surfaces perpendicular to the loading axis are parallel prior to testing. BN powders were used as lubricant to minimize friction between test samples and the compression platform. High temperature deformation tests were conducted using an Instron 5500R type machine equipped with a high temperature furnace capable of maintaining a temperature fluctuation within ±1 K. In order to shorten the time for heating the

* Corresponding author at: School of Materials Science and Engineering, Harbin Institute of Technology, West Dazhi Street 92, Harbin, Heilongjiang Province 150001, China. Tel.: +86 451 86403195; fax: +86 451 86403196.
E-mail address: yjhuanghit@yahoo.com.cn (Y. Huang).

0925-8388/$ – see front matter © 2010 Elsevier B.V. All rights reserved.
doi:10.1016/j.jallcom.2010.02.163

sample, the compressive jig was preheated to the pre-determined test temperature. Once the target temperature was reached, a sample was then rapidly placed into the holder load train and held for about 500 s to stabilize its temperature before loading.

3. Results and discussion

Strain rate often has a significant effect on the high temperature deformation response of amorphous metals [5]. Fig. 1 shows a representative series of true stress–true strain curves obtained from the deformation of the Ti-based BMG alloy at different test temperatures and a variety of applied strain rates. At 613 K, four typical strain rates of 1.3×10^{-4}, 4.0×10^{-4}, 1.0×10^{-3}, and 3.0×10^{-3} s^{-1} were selected and the corresponding true stress–true strain curves are shown in Fig. 1a. For the case of $\dot{\varepsilon} = 3 \times 10^{-3}$ s^{-1} at 613 K, 1.0×10^{-2} s^{-1} at 628 K, 3.0×10^{-2} s^{-1} at 643 K, a brittle fracture at maximum strength without macroscopic plasticity, indicating inhomogeneous deformation, can be identified. For the smaller strain rates, the true stress–true strain curves are characterized by a stress overshoot in the initial stage of deformation followed by a steady-state flow with a stress plateau in the extended strain region. The peak of the stress overshoot decreased monotonically as the strain rate decreased. The stress overshoot as a transient phenomenon has been reported to occur in Zr-based [5,7], and Mg-based [9] bulk metallic glasses and has been attributed to a change in atomic mobility because of a rapid change of free volume [6]. Interestingly, the curves at test temperatures of 628 and 643 K under the strain rate of 1.3×10^{-4} s^{-1} (the lowest strain rate used in the present work), show evidence of strain-hardening during the later stage of the deformation. A similar phenomenon has also been reported previously in Zr-based [6], Ca-based [19], and Cu-based [20] BMGs. Lower strain rate usually means that compressive deformation takes a longer time and the effect of high-ambient temperature on the amorphous phase is more serious. Thus, the strain-hardening resulting from the structural change of the amorphous phase occurs in the extended process of deformation [7]. At a test temperature of 658 K, within the strain rate range studied, no brittle fracture feature can be identified from the true stress–true strain curves. For strain rates of 1.0×10^{-2} and 3.0×10^{-2} s^{-1}, a characteristic stress overshoot evolves before the system reaches a steady-state. Meanwhile, lower strain rates, i.e., 3.0×10^{-3}, 1.0×10^{-3}, and 4.0×10^{-4} s^{-1}, promote homogeneous flow with a pronounced steady-state regime at a constant true stress. It should be noted that a significant compressive strain of 0.83 (not shown here) can be achieved after compressive deformation at 658 K with an applied strain rate of 3.0×10^{-3} s^{-1}. Such unique flowability for the alloy studied will enable precise shaping

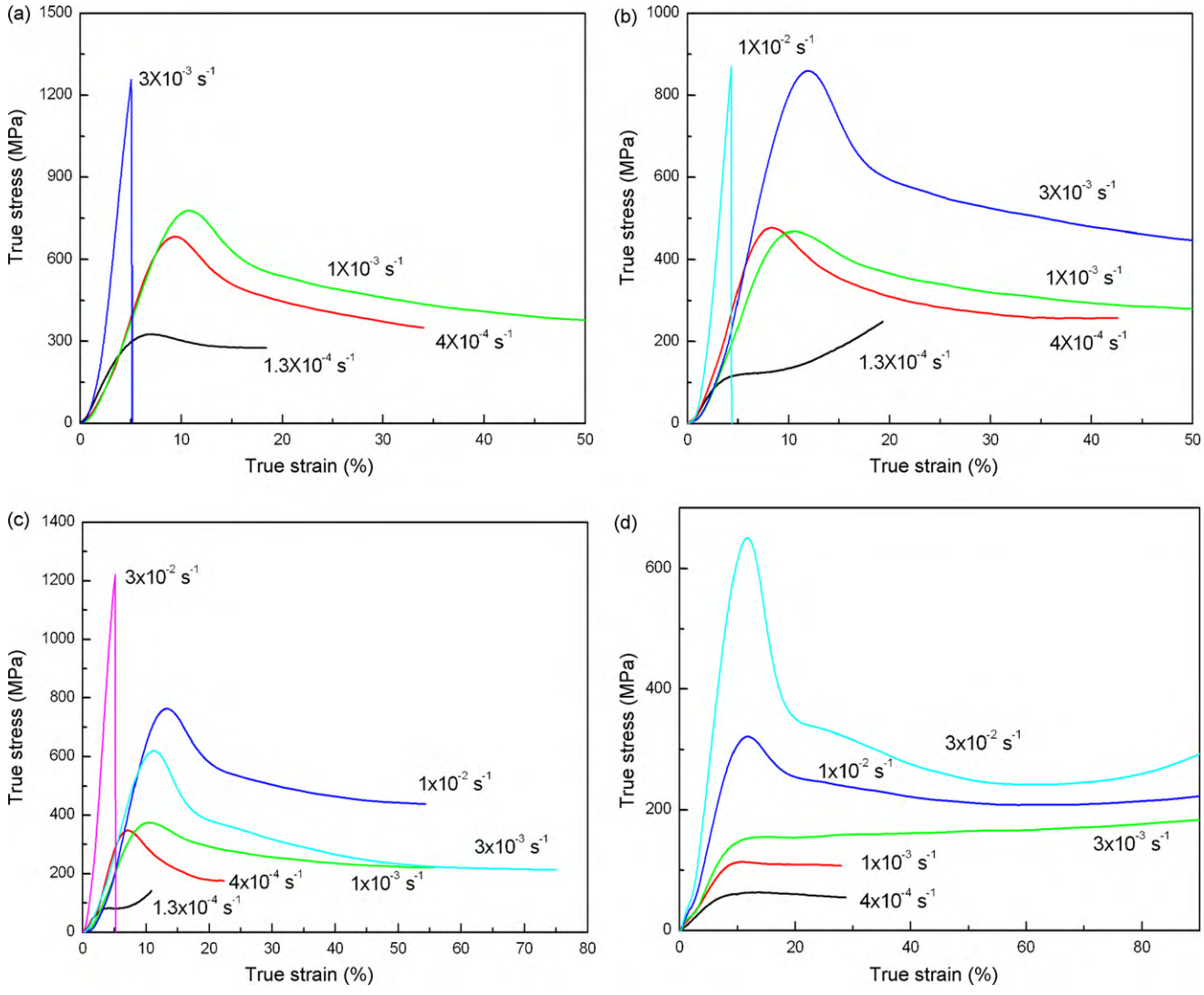

Fig. 1. Compressive true stress–true strain curves of $Ti_{40}Zr_{25}Ni_3Cu_{12}Be_{20}$ bulk metallic glass tested under various strain rates at different test temperatures: (a) 613 K, (b) 628 K, (c) 643 K, and (d) 658 K.

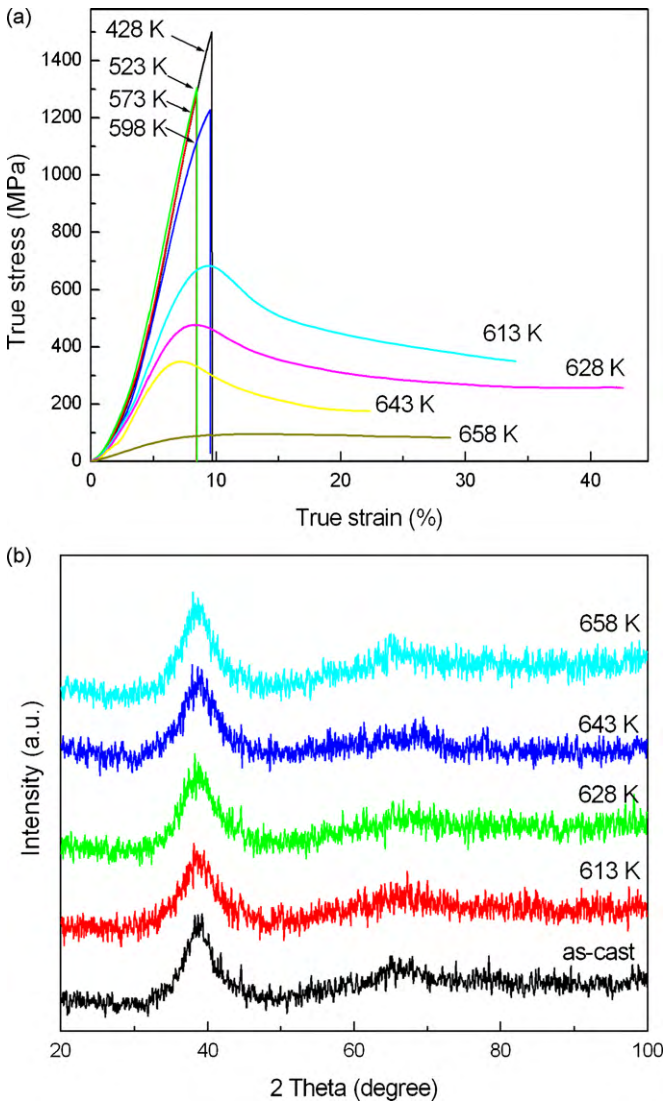

Fig. 2. (a) Compressive true stress–true strain curves of $Ti_{40}Zr_{25}Ni_3Cu_{12}Be_{20}$ bulk metallic glass tested at various test temperatures with a strain rate of 4×10^{-4} s^{-1} and (b) XRD patterns from $Ti_{40}Zr_{25}Ni_3Cu_{12}Be_{20}$ bulk metallic glass tested at various test temperatures with a strain rate of 4×10^{-4} s^{-1}, and in the as-cast condition.

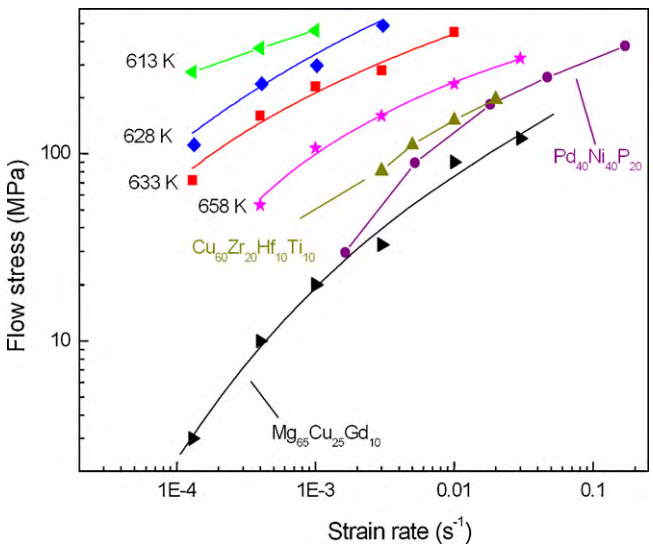

Fig. 3. Relationship between flow stress and strain rate tested at different test temperatures for $Ti_{40}Zr_{25}Ni_3Cu_{12}Be_{20}$ bulk metallic glass. Data from bulk $Pd_{40}Ni_{40}P_{20}$ glass at 590 K [21], $Cu_{60}Zr_{20}Hf_{10}Ti_{10}$ glass at 750 K [8], and $Mg_{65}Cu_{25}Gd_{10}$ glass at 328 K [22] are included for comparisons.

of complex parts, widening the range of its applications towards elevated temperature within SLR.

In addition to the strong strain rate dependence of the deformation of Ti-based glassy alloy studied, the test temperature dependence of the true stress–true strain curves has been also investigated. A typical example of the true stress–true strain curves is shown in Fig. 2a for a strain rate of 4.0×10^{-4} s^{-1} and different test temperatures. The true stress–true strain curves for the test temperatures lower than 613 K exhibit a linear relationship before failure, typical of brittle deformation behavior. As the test temperature increases, the maximum stress gradually decreases. When the test temperature is between 613 and 643 K, the deformation mode switched from being inhomogeneous (shear failure) to homogeneous. A characteristic stress overshoot can be identified before the system reaches a steady-state from the true stress–true curves. At 658 K, the stress increased monotonically as the strain increased until it reached a steady-state value and subsequently leveled off as the strain increased further.

Three different types of deformation modes can be identified from the above observations. The first mode is characterized by brittle fracture without appreciable plastic flow caused by shear localization at lower temperatures and higher strain rates. The second mode, i.e., steady-state flow after a stress overshoot, occurs at an intermediate temperature and strain rate region, while the third mode, i.e., large viscous flow without stress overshoot implying Newtonian viscous flow, is observed under the test conditions of lower strain rates and higher temperatures.

XRD patterns for the Ti-based BMG sample tested from 613 to 658 K with an applied strain rate of 4.0×10^{-4} s^{-1}, along with that from the as-cast sample are shown in Fig. 2b. Broad Bragg peaks with no detectable crystalline phases are observed, suggesting that the amorphous structure is the major phase in the tested alloy. Thus, the samples are essentially amorphous after testing within the supercooled liquid region at a strain rate of 4.0×10^{-4} s^{-1}.

To further discuss the flow behaviors of the BMG, the flow stress, which is defined as the peak-yield stress, as a function of the applied strain rate at various test temperatures is plotted in Fig. 3. The curves shift towards higher flow stress with decreasing test temperature. Fig. 4 shows plots of strain rate dependence of viscosity for the bulk Ti-based metallic glass studied. The viscosity, η, is calculated based on the following equation $\eta = \sigma/3\dot{\varepsilon}$ [5]. For the case of 658 K, at lower strain rate, such as 4.0×10^{-4} and 1.0×10^{-3} s^{-1}, the viscosity was essentially independent of the strain rate, indicating a linear relationship between flow stress and strain rate (i.e., Newtonian flow). At higher strain rate, however, there is a rapid decrease in the viscosity, and the viscosity is no longer a constant, demonstrating a transition from Newtonian flow to non-Newtonian flow. This tendency shifted towards higher strain rate and lower viscosity with increasing test temperature. At a low temperature of 613 K, the negative strain rate dependence of viscosity is strong within the applied strain rates, showing a non-Newtonian flow. For a direct comparison, results from $Pd_{40}Ni_{40}P_{20}$ [21], $Cu_{60}Zr_{20}Hf_{10}Ti_{10}$ [8], and $Mg_{65}Cu_{25}Gd_{10}$ [22] glasses are also included in Figs. 3 and 4. It is noted that flow stress of the Ti-based glass studied is larger than those of the Pd-based, Cu-based, and Mg-based glasses. On the other hand, under the proper testing conditions, the Pd-based, Cu-based, and Mg-based glasses exhibit a distinct transition from Newtonian to non-Newtonian flow, as indicated in Fig. 4. This is consistent with the observation of the Ti-based glass studied.

For the purpose of explaining the deformation trends of the metallic glass used in the study, a useful physical-based model, i.e., free volume model, was employed in the present work. The con-

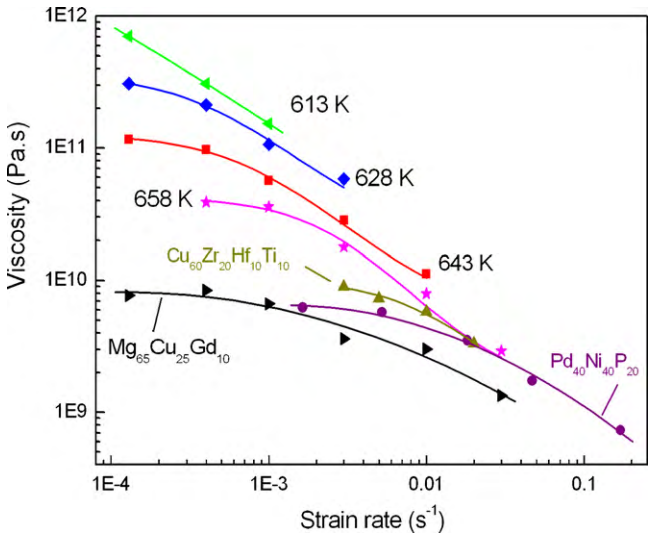

Fig. 4. Strain–stress dependence of the viscosity at various test temperatures for $Ti_{40}Zr_{25}Ni_3Cu_{12}Be_{20}$ bulk metallic glass. Data from bulk $Pd_{40}Ni_{40}P_{20}$ glass at 590 K [21], $Cu_{60}Zr_{20}Hf_{10}Ti_{10}$ glass at 750 K [8], and $Mg_{65}Cu_{25}Gd_{10}$ glass at 328 K [22] are included for comparisons.

Table 1
Reference strain rates and activation volumes for various test temperatures.

Test temperatures, K	$\dot{\varepsilon}_0$, s^{-1}	V_{act}, nm^3
658	8.4×10^{-4}	0.4127
643	4.3×10^{-4}	0.2620
628	2.4×10^{-4}	0.1832
613	1.5×10^{-4}	0.1502

cept of free volume has been proposed initially for liquid structures by Cohen and Turnbull [23] and has been extended by Spaepen [24] for plastic flow of amorphous metal materials. Free volume in amorphous structure is defined as excess volume compared to an ideal disordered atomic configuration of maximum density. For the case of high temperature deformation of metallic glasses, the free volume model provides a constitutive flow law written in terms of uniaxial stress σ and strain rate $\dot{\varepsilon}$ as $\dot{\varepsilon} = \dot{\varepsilon}_0 \sinh(\sigma V_{act}/2\sqrt{3}kT)$ [24], where k is Boltzmann's constant and T is temperature, at which the deformation is carried out, the activation volume V_{act}, as well as the reference strain rate $\dot{\varepsilon}_0$ is used as fitting parameters for adapting the model curves to the experiment data. Both V_{act} and $\dot{\varepsilon}_0$ for a given test temperature can be obtained by fitting the experiment values of stresses and strain rates using the above equation, and the corresponding results are listed in Table 1. As can be seen, at 658 K, the value of the activation volume V_{act} is about 0.4127 nm^3 and this is reduced to 0.1502 nm^3 at 613 K, with values of $\dot{\varepsilon}_0$ ranging from 1.5×10^{-4} to 8.0×10^{-4} s^{-1}. Such volumes is of about the same order of magnitude as that suggested by Argon for binary Pd–Si glass [25] and also comparable to more recent estimates for Zr-based [26], Pd-based [27], La-based [28], Mg-based [9] metallic glasses and Zr-based metallic glass matrix composites [29,30]. It can also be clearly seen from Table 1 that V_{act} decreases with decreasing test temperatures. During the high temperature deformation of metallic glass, with an increase in the test temperature, the viscosity of the BMG drops and consequently the fluidity increases, leading to higher value for activation volume for higher test temperatures.

4. Conclusions

The excellent plastic deformation behavior of a TiZrNiCuBe glassy alloy in the supercooled liquid region has been demonstrated. A large compressive strain of 0.83 can be achieved at 658 K and a strain rate of 3.0×10^{-3} s^{-1}. Plastic flow of supercooled liquid depends strongly on both applied strain rate and test temperature. The supercooled liquid behaves like a Newtonian fluid at high temperatures and low strain rates. However, non-Newtonian flow dominates during deformation at low temperatures and high strain rates.

Acknowledgements

This work was supported by the National Natural Science Foundation of China (NSFC) under Grant nos. 50904021, 50871034, and 10732010, the Foundation of China Postdoctor under Grant no. 20090450999, Excellent Youth Foundation of Heilongjiang Province under Grant no. JC200806, Key Laboratory Opening Funding of HIT.KLOF.2009007 (Key Laboratory of Micro-systems and Micro-structures Manufacturing (Harbin Institute of Technology), Ministry of Education, China), and the Hi-Tech Research and Development Program of China (Project no. 2007AA03Z518).

References

[1] A.L. Greer, Science 267 (1995) 1947.
[2] W.H. Wang, C. Dong, C.H. Shek, Mater. Sci. Eng. R44 (2005) 45.
[3] A.R. Yavari, J.J. Lewandowski, J. Eckert. MRS Bull. 32 (2007) 635.
[4] C.A. Schuh, T.C. Hufnagel, U. Ramamurty, Acta Mater. 55 (2007) 4067.
[5] J. Lu, G. Ravichandran, W.L. Johnson, Acta Mater. 51 (2003) 3429.
[6] T.G. Nieh, J. Wadsworth, Scr. Mater. 54 (2006) 387.
[7] G. Wang, J. Shen, J.F. Sun, Y.J. Huang, J. Zou, Z.P. Lu, Z.H. Stachurski, B.D. Zhou, J. Non-Cryst. Solids 351 (2005) 209.
[8] C.L. Chiang, J.P. Chu, C.T. Lo, T.G. Nieh, Z.X. Wang, W.H. Wang, Intermetallics 12 (2004) 1057.
[9] B. Gun, K.J. Laws, M. Ferry, Mater. Sci. Eng. A471 (2007) 130.
[10] Y. Kawamura, T. Shibata, A. Inoue, T. Masumoto, Acta Mater. 46 (1998) 253.
[11] G. Kumar, H.X. Tang, J. Schroers, Nature 451 (2009) 868.
[12] J.P. Chu, H. Wijaya, C.W. Wu, T.R. Tsai, C.S. Wei, T.G. Nieh, J. Wadsworth, Appl. Phys. Lett. 90 (2007) 034101.
[13] Y. Saotome, Y. Fukuda, I. Yamaguchi, A. Inoue, J. Alloys Compd. 434–435 (2007) 97.
[14] J.F. Sun, Y.J. Huang, J. Shen, G. Wang, D.G. McCartney, J. Alloys Compd. 415 (2006) 198.
[15] C.T. Pan, T.T. Wu, M.F. Chen, Y.C. Chang, C.J. Lee, J.C. Huang, Sens. Actuators A 141 (2008) 422.
[16] G. Kumar, J. Schroers, Appl. Phys. Lett. 92 (2008) 031901.
[17] Y.J. Huang, J. Shen, J.F. Sun, Appl. Phys. Lett. 90 (2007) 081919.
[18] Y.J. Huang, J. Shen, J.F. Sun, Z.F. Zhang, Mater. Sci. Eng. A 498 (2008) 203.
[19] K.J. Laws, B. Gun, M. Ferry, Mater. Sci. Eng. A480 (2008) 198.
[20] W.J. Kim, Y.K. Sa, J.B. Lee, H.G. Jeong, Intermetallics 14 (2006) 1391.
[21] Y. Kawamura, T. Nakamura, A. Inoue, Scr. Mater. 39 (1998) 301.
[22] Y.J. Huang, J. Shen. Unpublished data.
[23] M.H. Cohen, D. Turnbull, J. Chem. Phys. 31 (1959) 1164.
[24] F. Spaepen, Acta Metall. 25 (1977) 407.
[25] A.S. Argon, Acta Metall. 27 (1979) 47.
[26] M. Bletry, P. Guyot, J.J. Blandin, J.L. Soubeyroux, Acta Mater. 54 (2006) 1257.
[27] P. de Hey, J. Sietsma, A. van den Beukel, Acta Mater. 46 (1998) 5873.
[28] B. van Aken, P. de Hey, J. Sietsma, Mater. Sci. Eng. A 278 (2000) 247.
[29] X.L. Fu, Y. Li, C.A. Schuh, Acta Mater. 55 (2007) 3059.
[30] S.F. Guo, K.C. Chan, Q. Chen, J.J. Li, L. Liu, Scr. Mater. 60 (2009) 369.